DMD Fast Forward. Published on March 17, 2017 as DOI: 10.1124/dmd.116.074492
This article has not been copyedited and formatted. The final version may differ from this version.

Title

Increased Plasma Exposures of Conjugated Metabolites of Morinidazole in Renal Failure Patients: A Critical Role of Uremic Toxins

Fandi Kong, Xiaoyan Pang, Kan Zhong, Zitao Guo, Xiuli Li, Dafang Zhong, and Xiaoyan Chen

Shanghai Institute of Materia Medica, Chinese Academy of Sciences, Shanghai 201203, China (F.K., X.P., K.Z., Z.G., X.L., D.Z., X.C.)

University of Chinese Academy of Sciences, Beijing 100049, China (F.K., D.Z., X.C.)

DMD Fast Forward. Published on March 17, 2017 as DOI: 10.1124/dmd.116.074492
This article has not been copyedited and formatted. The final version may differ from this version.

Running title: Uremic toxins inhibit renal uptake of morinidazole conjugates

Corresponding author:

Xiaoyan Chen, Ph. D.

Shanghai Institute of Materia Medica, Chinese Academy of Sciences, 501 Haike Road, Shanghai 201203, China.

E-mail: xychen@simm.ac.cn

Number of text pages: 22

Number of tables: 5

Number of figures: 9

Number of references: 31

Number of words in Abstract: 246

Number of words in Introduction: 767

Number of words in Discussion: 1313

Abbreviations: AUC, area under the plasma concentration-time curve; BCA, bicinchoninic acid; BUN, blood urine nitrogen; CKD, chronic kidney disease; CMPF, 3-carboxy-4-methyl-5-propyl-2-furanpropionate; CRF, chronic renal failure; DEPC, diethyl pyrocarbonate; DMEM: Dulbecco's modified Eagle's medium; FBS, fetal bovine serum; GFR, glomerular filtration rate; HA, hippuric acid; HBSS, Hanks' balanced salt solution; HD, hemodialysis; HE stain, hematoxylin–eosin stain; HEK293, human embryonic kidney 293; HPLC, high-performance liquid chromatography; IAA, indole-3-acetic acid; IS, indoxyl

sulfate; LC-MS/MS, liquid chromatography-tandem mass spectrometry; OAT, organic anion transporter; PCR, polymerase chain reaction; SD rats, Sprague-Dawley rats; TLCA, taurolithocholic acid; UGTs, UDP-glucuronosyltransferases; 5/6 Nx rat, 5/6 nephrectomized rat.

DMD Fast Forward. Published on March 17, 2017 as DOI: 10.1124/dmd.116.074492
This article has not been copyedited and formatted. The final version may differ from this version.

ABSTRACT

Morinidazole is a 5-nitroimidazole drug. Its sulfate conjugate M7 was a sensitive substrate of organic anion transporter 1 (OAT1) and OAT3, whereas N^+-glucuronides M8-1 and M8-2 were only OAT3 substrates. In chronic renal failure (CRF) patients, plasma exposures of the three conjugates increased by 15-fold, which were also found in 5/6 nephrectomized (5/6 Nx) rats in this study. Although the transcriptions of Oat1 and Oat3 in 5/6 Nx rat kidneys decreased by 50%, no difference was observed on the three conjugate uptakes between control and 5/6 Nx rat kidney slices. Thus, the highly elevated endogenous uremic toxins in 5/6 Nx rats and humans, namely, 3-carboxy-4-methyl-5-propyl-2-furanpropionate (CMPF), hippuric acid (HA), and indoxyl sulfate (IS), were considered as influential factors. In rat kidney slices, uptakes of M7, M8-1, and M8-2 were dose-dependently reduced by HA and IS, whose plasma concentrations were elevated five times in 5/6 Nx rats. In OAT3-overexpressed cells, the three conjugate uptakes were inhibited by CMPF, HA, and IS with IC_{50} values of 19.2, 87.4, and 222 μM (M7); 8.53, 39.4, and 161 μM (M8-1); and 6.75, 24.1, and 78.3 μM (M8-2), respectively. In OAT1-overexpressed cells, CMPF, HA, and IS showed weak inhibition on M7 uptake with IC_{50} values of 187, 162, and 200 μM, correspondingly. Results suggest that the reduced mRNA expression of renal transporters in CRF patients may not influence the activities of these transporters. However, accumulated uremic toxins may inhibit the transporters, particularly OAT3, leading to plasma exposure changes of relevant substrates.

DMD Fast Forward. Published on March 17, 2017 as DOI: 10.1124/dmd.116.074492
This article has not been copyedited and formatted. The final version may differ from this version.

Introduction

Chronic kidney diseases (CKDs) are major chronic illnesses primarily threatening public health, as reported by WHO in 2012 (Moll et al., 2014). The absorption, distribution, metabolism, and extraction processes of drugs differ in patients with chronic renal failure (CRF), and dose adjustment should be considered in clinical uses (Verbeeck and Musuamba, 2009). CRF can reduce the renal clearance of drugs by decreasing the glomerular filtration rate (GFR) (Naud et al., 2011). For example, the pharmacokinetic characteristic of memantine changed with varying GFR in CRF patients, and the dose was reduced in half for severe renal impairment patients (Periclou et al., 2006). Renal dysfunction can also affect the expression and functions of kidney transporters (Verbeeck and Musuamba, 2009; Naud et al., 2011; Schwenk and Pai, 2016). Sakurai et al. (Sakurai et al., 2004) showed that human organic anion transporter 1 (OAT1) and OAT3 mRNA levels in the kidneys of patients with renal diseases were lower than those in normal kidneys; they demonstrated that the elimination constant of cefazolin, a substrate of OAT3, was significantly correlated with OAT3 mRNA levels in humans. More direct evidences from *Oat1*-knockout and *Oat3*-knockout mice have shown impaired handling of small anionic drugs and their metabolites (Nigam, 2015). The down-regulations of organic anion transporters could lead to the accumulation of uremic toxins (Wikoff et al., 2011), which caused uremic syndrome and affected the transport of drugs and their metabolites in CRF patients (Deguchi et al., 2004). These uremic toxins are categorized into small free water-soluble compounds, middle molecules, and protein-bound solutes (Vanholder et al., 2003). Protein-bound solutes, such as indoxyl sulfate (IS), 3-carboxy-4-methyl-5-propyl-2-furanpropionate (CMPF), hippuric acid (HA), and

DMD Fast Forward. Published on March 17, 2017 as DOI: 10.1124/dmd.116.074492
This article has not been copyedited and formatted. The final version may differ from this version.

indole-3-acetic acid (IAA), cannot be completely removed by hemodialysis (HD) (Sarnatskaya et al., 2002); therefore, their plasma levels increased by 10–100 times in patients with renal impairment (Vanholder et al., 2003; Fujita et al., 2011; Itoh et al., 2012). CMPF was the substrate of OAT3, whereas OAT1 mainly accounted for HA and IAA uptakes; OAT1 and OAT3 equally contributed to the renal uptake of IS (Deguchi et al., 2004). Thus, OAT1 and OAT3 may affect the renal clearance of drugs and metabolites that are substrates of these kidney transporters.

Morinidazole, *R*,*S*-1-(2-methyl-5-nitro-1*H*-imidazol-1-yl)-3-morpholinopropan-2-ol, is a novel 5-nitroimidazole antimicrobial drug approved for treating amoebiasis, trichomoniasis, and anaerobic bacterial infections (Gao et al., 2011). This drug exhibited greater antiparasitic activity with less toxicity in preclinical and *in vitro* studies than metronidazole (Gao et al., 2011). Following an intravenous infusion in humans, morinidazole was primarily metabolized via N^+-glucuronidation forming the N^+-glucuronide of *S*-morinidazole M8-1 and N^+-glucuronide of *R*-morinidazole M8-2, as well as *O*-sulfation forming the sulfate conjugate M7 (Fig. 1) (Gao et al., 2011). Morinidazole and its conjugates M7, M8-1, and M8-2 were mainly excreted through the urine, accounting for 21.2%, 13.0%, 6.6%, and 28.4% of the dose (Zhong et al., 2014). The $AUC_{0\text{-}t}$ values of conjugates M7, M8-1, and M8-2 in severe renal impairment patients were 15.1-, 20.4-, and 17.4-fold higher than those in healthy subjects with the same dose, whereas the $AUC_{0\text{-}t}$ value of the parent drug was only 1.5-fold higher (Zhong et al., 2014). M7 was a sensitive substrate of two renal transporters, namely, OAT1 and OAT3; M8-1 and M8-2 were the only substrates of OAT3 (Zhong et al., 2014). Therefore, it was speculated that the significant elevation in the plasma exposures of conjugated

DMD Fast Forward. Published on March 17, 2017 as DOI: 10.1124/dmd.116.074492
This article has not been copyedited and formatted. The final version may differ from this version.

metabolites may be mediated by the altered expression or activities of OAT1 and OAT3 in the kidneys of patients with renal impairment. In terms of uptake clearance (V_{max}/K_m, where V_{max} is the maximum uptake rate, and K_m is the Michaelis–Menten constant), OAT1 (17.0 μL/min/mg protein) and OAT3 (16.0 μL/min/mg protein) presented similar contributions to the renal uptake of M7 (Zhong et al., 2014). Additionally, the V_{max}/K_m of M7 by OAT3 was higher than that of M8-1 (1.0 μL/min/mg protein) and M8-2 (1.7 μL/min/mg protein), indicating that M7 is a more sensitive substrate for OAT3 than glucuronide conjugates (Zhong et al., 2014). If the increase in the plasma exposure is only mediated by the altered expression of transporters, the change of M7 caused by OAT1 and OAT3 should be significantly higher than that of M8-1 or M8-2 caused only by OAT3. However, the concentration increase of three conjugates was similar. Hence, we hypothesized that some other mechanisms accounted for the boosted plasma exposures of morinidazole-conjugated metabolites in severe renal failure patients; for instance, accumulated uremic toxins may affect the renal uptake of the conjugates.

The 5/6 nephrectomized (5/6 Nx) rat model was characterized by hyperfiltration in the remaining nephrons (Anderson et al., 1985), which was employed to mimic CRF in humans. Naud et al. (Naud et al., 2011) showed a decrease in protein (40%) and mRNA (75%) expression for Oat1, as well as reduced protein (87%) and mRNA (70%) expression for Oat3 in the kidneys of rats 41 days post-5/6 nephrectomy. In the 5/6 nephrectomized rats, both uremic toxins IS and HA significantly increased (Kikuchi et al., 2010), similar to that in CRF humans. Therefore, this study used the 5/6 nephrectomized rats for *in vivo* and *in vitro* experiments, such as kidney slices. In addition, OAT1 or OAT3 overexpressed human

DMD Fast Forward. Published on March 17, 2017 as DOI: 10.1124/dmd.116.074492
This article has not been copyedited and formatted. The final version may differ from this version.

embryonic kidney 293 (HEK293) cells were also used to investigate the mechanism of the increased plasma exposures of morinidazole conjugates in renal failure patients.

DMD Fast Forward. Published on March 17, 2017 as DOI: 10.1124/dmd.116.074492
This article has not been copyedited and formatted. The final version may differ from this version.

Materials and methods

Chemicals

Morinidazole raceme (99.9% purity) was kindly provided by Jiangsu Hansoh Pharmaceutical Co. Ltd. (Liangyungang, China). N^+-glucuronide of *S*-morinidazole M8-1 and N^+-glucuronide of *R*-morinidazole M8-2 were isolated and purified from human urine as previously described (Gao et al., 2011). Sulfate conjugate of morinidazole M7 was synthesized as previously described with minor modifications (Shrestha et al., 2011). HA and IAA were purchased from J&K Scientific Ltd. (Beijing, China). Salicylic acid was purchased from Meilun Biology Technology Co. Ltd. (Dalian, China). Indoxyl sulfate potassium salt, sodium pentobarbital, metronidazole, probenecid, Hanks' balanced salt solution (HBSS), and hygromycin B were obtained from Sigma-Aldrich (St. Louis, MO, USA). CMPF was obtained from Toronto Research Chemicals (North York, Canada). Bicinchoninic acid (BCA) protein assay kit was purchased from Beyotime (Jiangsu, China). Assay kits of creatinine, urine protein, and blood urine nitrogen (BUN) were supplied by Nanjing Jiancheng Bioengineering Institute (Jiangsu, China). TRIzol regent, diethyl pyrocarbonate (DEPC) treated water, Dulbecco's modified Eagle's medium (DMEM), fetal bovine serum (FBS), 0.05% trypsin-EDTA, penicillin G, streptomycin, and SuperScript III reverse transcriptase kit were purchased from Invitrogen (Carlsbad, CA, USA). Deionized water was obtained using a Millipore Milli-Q gradient water purification system (Molsheim, France). All other solvents and regents were of either high-performance liquid chromatography (HPLC) or analytical grade.

Construction of 5/6 Nx rat model

All procedures involving animals were performed in accordance with *Guide for the Care and*

Use of Laboratory Animals of the Shanghai Institute of Materia Medica, Chinese Academy of Sciences. Male Sprague-Dawley (SD) rats weighing 180 g to 220 g were allowed an acclimatization period of at least 7 days before the first nephrectomy. CRF was induced by two-stage 5/6 nephrectomy as previously described (Deguchi et al., 2003). Following anesthesia with sodium pentobarbital (50 mg/kg) by intraperitoneal injection, the left kidney was exposed to excise the upper and lower poles of about 1/3. After 7 days, rats were anesthetized again, and the whole right kidney was removed. Control rats were subjected to sham operations identical to those used for 5/6 Nx rats except that the kidneys or renal poles were not removed. All rats were allowed free access to water, and control rats were fed the same amount of fodder that 5/6 Nx rats consumed on the previous day to reduce the imbalance on the weights (Naud et al., 2011). At 41 days after nephrectomy, urine was collected for 24 h to determine the clearance of creatinine and urine protein. Blood samples were allowed to stand for 30 min and then centrifuged at 11000 rpm for 5 min to obtain serum samples for measurement of serum creatinine and BUN.

Pharmacokinetic experiments

Animals were fasted for 12 h with free access to water before the experiments. Morinidazole was administered intravenously via the tail to 5/6 Nx rats (n=11) and control rats (n=6) at a dose of 50 mg/kg. Blood samples were collected from retro-orbital venous plexus pre-dosage (0 h), at 5, 15, and 30 min, as well as at 1, 2, 4, 6, 8, and 12 h post-dosage in tubes containing an anticoagulant. Plasma samples were centrifuged at 11000 rpm for 5 min at 4°C and then stored at −20°C until analysis. Following the pharmacokinetic experiments, rats were anesthetized immediately for excision of the remnant kidneys of 5/6 Nx rats and the left

kidneys of control rats. Each kidney was divided into two parts: one part was fixed in 4% formalin for hematoxylin–eosin (HE) stain, and the other part was frozen immediately in liquid nitrogen and then stored at −80°C.

To investigate the pharmacokinetics of M7, 5/6 Nx rats (n=13) and control rats (n=9) were intravenously injected into the tail vein at a dose of 15 mg/kg. Blood samples were collected pre-dosage (0 h), at 5, 15, 30, and 45 min, as well as at 1, 1.5, and 2 h post-dosage. Plasma samples were harvested and tissue samples were processed the same as above.

Before the pharmacokinetic experiment of M7 in 5/6 Nx rats, the dose dependency of M7 pharmacokinetic parameters was examined in normal SD rats. Twelve normal SD rats were randomly divided into three groups. M7 was administrated intravenously via the tail vein with different doses: 0.1, 1.5, and 15 mg/kg. Blood samples were collected at 5, 15, 30, and 45 min, as well as 1, 1.5, and 2 h after dose administration. Plasma samples were harvested as above.

Tissue distribution

Normal SD rats (n=24) weighing 180 g to 220 g were randomly divided into two groups, which were fasted for 12 h with free access to water before the experiments. Morinidazole was administered intravenously via tails of twelve rats at a dose of 50 mg/kg, and M7 was administered intravenously to another twelve rats at a dose of 15 mg/kg. At 0.25, 0.75, and 1.50 h after dose administration, rats (n=4 at each time point in each group) were sacrificed via exsanguination from the abdominal aorta under anesthesia. Livers, kidneys, lungs, hearts, and spleens were rapidly dissected, washed with saline, dried, and weighed. Every 200 mg of the tissue samples was homogenized with 1 mL of saline and stored at −20°C until analysis. Blood samples were collected and centrifuged to harvest plasma samples. All plasma samples

DMD Fast Forward. Published on March 17, 2017 as DOI: 10.1124/dmd.116.074492
This article has not been copyedited and formatted. The final version may differ from this version.

were stored at −20°C.

Biochemistry and histopathological examination

Urine creatinine and protein, serum creatinine, and BUN were determined using the corresponding assay kits in accordance with the manufacturer's instruction. Formalin-fixed tissues were embedded in paraffin, cut into slices, and stained with HE. HE sections were observed with optical microscopy.

mRNA analysis

RNAs of renal cortex were extracted using TRIzol regent. cDNA was synthesized from 1 μg of total RNA by using SuperScript^{TM} III reverse transcriptase kit [synthesis primers were oligo (dT)]. The reaction was performed in a volume of 10 μL, containing 25 ng/μL cDNA, 250 nM corresponding primer, and 5 μL of QuantiFast SYBR Green PCR Master Mix (Qiagen, Germany) on an ABI7500 Fast Real-Time PCR system (Applied Biosystems, Foster City, CA, USA). qPCR conditions were 95°C for 10 min, 95°C for 15 s, and 57.5°C for 60 s for 40 cycles. The sequences of primers were as follows: Oat1 (forward) 5'-ACCCCACAGTGATTCGGCAG-3', (reverse) 5'-GGCATGGAGGGGTAGAACTC-3'; Oat3 (forward) 5'-CAGTTTTGGTTCATCTTGCCTGGTG-3', (reverse) 5'-CCAGCAAGGTCACATGCAGGTA-3'; and β-actin (forward) 5'-GCCACCAGTTCGCCAT-3', (reverse) 5'-CATACCCACCATCACACC-3'. PCR products were analyzed using ΔΔCt (Livak and Schmittgen, 2001) with β-actin as internal standard.

Kidney slices

Kidney slices were experimented as previously described (Obatomi et al., 1998). Rats were sacrificed via exsanguination from the abdominal aorta under anesthesia, and the kidneys

were excised. The kidneys were decapsulated and cored (8 mm i.d.) perpendicular to the cortico-papillary axis. Kidney slices with a thickness of 300 μm and a diameter of 8 mm were prepared in Krumdieck tissue slicer MD6000 (TSE systems, Chesterfield, MO, USA) with ice-cold and carbogen-statured (95% O_2, 5% CO_2) Krebs-bicarbonate buffer (120 mM NaCl, 16.2 mM KCl, 10 mM Na_2HPO_4/NaH_2PO_4, 1.2 mM $MgSO_4$ and l mM $CaCl_2$, pH 7.5) (Habu et al., 2003). After 5 min preincubation at 37°C, kidney slices were transferred to 24 well-cultured plates containing 1 mL of buffer with test compounds for further incubation at 37°C. All the incubations were under a carbogen atmosphere. To study the effect of CRF on the uptake, kidney slices of 5/6 Nx rats (n=6) and control rats (n=4) were incubated with M7 (30 μM), M8-1 (100 μM), or M8-2 (100 μM). The uptake was measured at 5 and 15 min. To study the effect of uremic toxins on the uptake, kidney slices of normal rats were incubated with M7 (30 μM), M8-1 (100 μM), or M8-2 (100 μM) in the presence or absence of probenecid and individual or mixed HA and IS with different concentrations for 15 min. At the end of each incubation, kidney slices were washed thrice with ice-cold HBSS and dried using a filter paper. After weighing, each kidney slice was homogenized with 300 μL of saline. Conjugated metabolites were determined using LC-MS/MS.

Cell cultures

HEK293 cells overexpressed with human OAT1 or OAT3 and empty-vector-transfected control cells (mock) were established at HD Bioscience Co. Ltd. (Shanghai, China). The functions of the transporters in these cells were identified and validated using corresponding typical substrates and inhibitors. Cells were maintained in DMEM supplemented with 10% FBS, 100 units/mL penicillin G, 100 μg/mL streptomycin, and 100 μg/mL hygromycin B at

DMD Fast Forward. Published on March 17, 2017 as DOI: 10.1124/dmd.116.074492
This article has not been copyedited and formatted. The final version may differ from this version.

37°C in a humidified 5% CO_2 atmosphere. Cells were seeded into the wells of 24-well BD Biocoat poly-D-lysine-coated plates (BD Biosciences, Bedford, MA, USA) at a density of 2×10^5 cells/well. Uptake studies were conducted 2 days after seeding, when the cells had grown to confluence.

In vitro inhibition experiments of uremic toxins

Prior to *in vitro* uptake study, cells were rinsed thrice with prewarmed HBSS (37°C, pH 7.4) and preincubated in 300 μL HBSS for 10 min at 37°C. Equilibration HBSS was removed, and uptake experiments were initiated by the addition of 300 μL HBSS containing test compound, with or without uremic toxins. Uptake experiments were terminated at a specific time by removing the incubation buffer. Cells were then washed thrice with ice-cold HBSS and lysed with 200 μL of deionized water for multigelation. The protein content of the cell lysate was determined using the BCA protein assay kit. Cell samples were stored at −20°C until analysis.

Determination of morinidazole and its conjugated metabolites

A 25 μL aliquot of sample (plasma, tissue homogenate, or cell lysate) and 25 μL of internal standard (50 ng/mL metronidazole) were mixed with 150 μL of acetonitrile. After vortexing and centrifugation at 14000 rpm for 5 min, 10 μL of the supernatants were diluted 10-fold with methanol/water (1:1, vol/vol), whereas 2 μL was used for the determination of morinidazole or M7 via LC-MS/MS method (Gao et al., 2011; Zhong et al., 2014). The standard curves for morinidazole and M7 (high concentration) in plasma ranged from 10 ng/mL to 10000 ng/mL. Remnant supernatants were evaporated to dryness under a gentle stream of nitrogen at 40 °C, and residues were dissolved in 100 μL of methanol/water (1:1, vol/vol), 5 μL of which was used for the determination of M7, M8-1, or M8-2 via a

DMD Fast Forward. Published on March 17, 2017 as DOI: 10.1124/dmd.116.074492
This article has not been copyedited and formatted. The final version may differ from this version.

LC-MS/MS method (Zhong et al., 2014). The standard curves ranged from 0.100 ng/mL to 300 ng/mL for M7 (low concentration), M8-1, and M8-2.

Determination of uremic toxins

IS, CMPF, HA, and IAA were determined using a Shimadzu LC-30AD HPLC system (Kyoto, Japan) and an API6500 triple-quadrupole MS (Applied Biosystems, Ontario, Canada). Analyst 1.6 software (Applied Biosystems) was used for data acquisition and processing. Chromatographic separation was achieved on Venusil ASB-C18 (150 mm × 4.6 mm id, 5 μm; Angela Technologies Inc., Newark, DE, USA) at 40°C. The mobile phase was a mixture of 5 mM ammonium acetate (A) and methanol (B) at a flow of 0.8 mL/min. The gradient elution program began from 25% B, increased linearly to 90% B in the next 2.7 min, and maintained for 1.8 min; in the next 1 min, the gradient was reduced to 25% B linearly and maintained at 25% B until the gradient was stopped at 6 min. Multiple reaction monitoring (*m/z* 174.0 → 129.9 for IAA, *m/z* 178.0 → 133.9 for HA, *m/z* 212.0 → 131.8 for IS, *m/z* 239.0 → 194.9 for CMPF, and *m/z* 136.8 → 92.8 for salicylic acid as internal standard) was used in the negative electrospray ionization mode with an ion spray voltage of −4000 V and a source temperature of 550 °C. The nebulizer gas, heater gas, and curtain gas were set to 50, 80, and 25 psi, respectively. The standard curve ranges were 0.100 to 30 μM for IAA and CMPF in plasma and 1.00 to 200 μM for IS and HA.

A 25 μL aliquot sample (plasma or homogenate of 200 mg kidney/mL saline) and 25 μL of internal standard (2 μg/mL salicylic acid) were mixed with 75 μL of acetonitrile containing 1% formic acid. After vortexing and centrifugation at 14000 rpm for 5 min, supernatants were diluted fourfold with initial mobile phase to measure IAA and CMPF and then diluted 40

DMD Fast Forward. Published on March 17, 2017 as DOI: 10.1124/dmd.116.074492
This article has not been copyedited and formatted. The final version may differ from this version.

times to measure HA and IS through LC-MS/MS analysis.

Data analysis

WinNonlin (version 6.1, Pharsight Corp, Cary, NC, USA) was used to calculate the pharmacokinetic parameters in a non-compartmental model. GraphPad Prism (version 6.0, GraphPad Software Inc., San Diego, CA, USA) was used to calculate the half inhibitory concentration (IC_{50}). All data were expressed as mean ± standard deviation (SD). Student's two-tailed unpaired *t*-test in SPSS (version 20.0, SPSS Inc., Chicago, IL, USA) was used to determine the difference. The level of statistical significance was set at $p < 0.05$.

The substrate uptake rate was normalized using the protein concentration of the cell lysate. The transporter-mediated uptake was obtained by subtracting the accumulation in the HEK293 cells of mock from that in the parallel uptake experiments in OAT-transfected HEK293 cells.

In the inhibition study, IC_{50} values were calculated by plotting the log value of inhibitor concentration against the normalized response as follows: $Y = 100 / \left[1 + 10^{(X\text{-}LogIC_{50})}\right]$

DMD Fast Forward. Published on March 17, 2017 as DOI: 10.1124/dmd.116.074492
This article has not been copyedited and formatted. The final version may differ from this version.

Results

Biochemistry parameters and histopathological sections of control and 5/6 Nx rats

Table 1 presents the biochemistry parameters of control and 5/6 Nx rats. Serum creatinine and BUN in 5/6 Nx rats increased to 2.88-fold ($p < 0.01$) and 7.10-fold ($p < 0.001$) of those in control rats, respectively. By contrast, creatinine clearance in 5/6 Nx rats decreased by 73.5% ($p < 0.05$). In the HE-stained sections (Fig. 2), partial glomerular enlargement and increased cells in glomus were observed in 5/6 Nx rats (Fig. 2C). The tubules were dilated with tubular lumina containing proteinaceous casts, and the epithelial cells swelled in 5/6 Nx rats (Fig. 2D).

Pharmacokinetics and tissue distribution

Plasma concentration–time curves of morinidazole and its conjugated metabolites after an intravenous injection of 50 mg/kg morinidazole to control and 5/6 Nx rats are shown in Fig. 3. Pharmacokinetic parameters are listed in Table 2. The AUC_{0-t} value and plasma clearance for morinidazole were similar in both groups. However, the AUC_{0-t} values for morinidazole-conjugated metabolites in 5/6 Nx rats significantly increased to 12.9-fold (M7), 10.7-fold (M8-1), and 14.0-fold (M8-2) of those in control rats.

Fig. 4 presents the plasma concentration–time curve of sulfate conjugate M7 after direct intravenous administration of 15 mg/kg M7 to control and 5/6 Nx rats; corresponding pharmacokinetic parameters are given in Table 3. The AUC_{0-t} value for M7 in 5/6 Nx rats was 3.61-fold higher than that of control rats, whereas the plasma clearance for M7 decreased to 27.8% in 5/6 Nx rats.

The dose dependency of M7 pharmacokinetic parameters was examined in normal SD rats

DMD Fast Forward. Published on March 17, 2017 as DOI: 10.1124/dmd.116.074492
This article has not been copyedited and formatted. The final version may differ from this version.

(Table 4). The increased AUC_{0-t} values of M7 were proportional to the doses from 0.15 mg/kg to 15 mg/kg, indicating that renal clearance of M7 at dose of 15 mg/kg was not saturated in rats.

The tissue distributions of M7 in normal rats after intravenous administration of morinidazole or M7 are shown in Fig. 5. After direct intravenous injection of M7, the kidney was the preferred site for disposition with the concentration 4.40-fold higher than that in the plasma at 0.25 h post dose. Concentration of M7 in the kidney at 1.50 h post dose was less than 1% of that at 0.25 h, indicating a low tissue retention (Fig. 5B). Following the intravenous injection of morinidazole, the relatively high concentrations of M7 were observed in the liver and kidney and lasted a relatively long period of time (Fig. 5A), probably because M7 was formed through the sulfation of the parent drug in these tissues.

mRNA expression of Oat1 and Oat3 in control and 5/6 Nx rat kidneys

Fig. 6 presents the mRNA expression of Oat1 and Oat3 in control and 5/6 Nx rats. There were significant decreases in the mRNA expression of Oat1 (49.3%, $p < 0.001$) and Oat3 (43.8%, $p < 0.001$) in 5/6 Nx rat kidneys compared with those in control rats. The relevance was investigated between mRNA expression and plasma exposure after direct intravenous administration of M7 to exclude the influence of individual difference in metabolism. Moderate correlations were observed between the AUC_{0-t} values of M7 and mRNA expression of Oat1 (coefficient $r = -0.7241$, $p < 0.001$) (Fig. 6C), as well as mRNA expression of Oat3 ($r = -0.6482$, $p < 0.001$) (Fig. 6D).

Uremic toxins in control and 5/6 Nx rats

In control and 5/6 Nx rats, only three of the four uremic toxins were observed, namely, IS, HA,

and IAA. The plasma and kidney concentrations of IS, HA, and IAA at 2 hour post dose were shown in Fig 7. The concentrations of IS increased to 4.93- and 5.67-fold in the plasma and kidneys of 5/6 Nx rats, whereas the concentrations of HA increased to 4.87- and 6.85-fold compared with those in control rats. The concentrations of IAA were low in both control and 5/6 Nx rats but remained constant in plasma and slightly decreased in 5/6 Nx rat kidneys. The relevance between uremic toxin plasma concentration and plasma exposure of M7 after direct intravenous administration was investigated to exclude the influence of individual difference in metabolism. The AUC_{0-t} values of M7 increased with the elevation of plasma concentrations of IS and HA. A correlation between the AUC_{0-t} values of M7 and plasma concentrations of IS was observed with a coefficient r of 0.9151 ($p < 0.001$) (Fig. 7B). A correlation between the AUC_{0-t} values of M7 and plasma concentrations of HA (r = 0.7788, $p < 0.001$) (Fig. 7D) was also determined. No correlation was found between the AUC_{0-t} values of M7 and plasma concentration of IAA (r = 0.2185, $p = 0.3286$) (Fig. 7F).

Uptake of morinidazole-conjugated metabolites in kidney slices

The uptakes for 5 and 15 min of the three conjugated metabolites, M7, M8-1, and M8-2, in the control and 5/6 Nx kidney slices are shown in Fig. 8 (A, B, and C). Data revealed that the conjugate accumulations showed no significant difference between control and 5/6 Nx kidney slices, irrespective of incubation period. In normal rat kidney slices, the uptakes of M7, M8-1, and M8-2 were investigated with different degrees of IS, HA and their mixture. With the concentration of 20, 100, and 500 μM IS, the uptake of M7 decreased to 91.3%, 63.5%, and 57.3%; M8-1 to 98.0%, 79.7%, and 68.0%; and M8-2 to 90.7%, 73.0%, and 50.0%, respectively. With the concentration of 20, 100, and 500 μM HA, the uptake of M7 was

DMD Fast Forward. Published on March 17, 2017 as DOI: 10.1124/dmd.116.074492
This article has not been copyedited and formatted. The final version may differ from this version.

decreased to 78.3%, 65.0%, and 38.7%; M8-1 to 87.3%, 80.3%, and 63.0%; and M8-2 to 99.5%, 81.0%, and 72.0%, respectively. The two uremic toxin mixtures of 20/20, 100/100, and 500/500 μM decreased the uptake of M7 to 78.4%, 60.7%, and 41.0%; M8-1 to 73.5%, 46.2%, and 33.3%; and M8-2 to 88.2%, 67.3%, and 57.2%, respectively (Fig. 8D, 8E, and 8F). The inhibitory effect of 200 μM probenecid was also examined, which decreased the uptake of morinidazole conjugates to 54.0% (M7), 31.0% (M8-1); and 32.0% (M8-2), respectively.

Inhibition of four uremic toxins for the uptakes of morinidazole-conjugated metabolites in OAT1/OAT3 overexpressed HEK293 cells

The inhibitory effects of probenecid and different concentrations of uremic toxin mixture on the uptake of M7, M8-1, and M8-2 were evaluated (Supplemental Fig. 1). The inhibitory effect of individual uremic toxin, CMPF, HA, IS and IAA was independently investigated. The four uremic toxins inhibited OAT1-mediated uptake of M7 and OAT3-mediated uptakes of three conjugated metabolites in a concentration-dependent manner (Fig. 9); the IC_{50} values are listed in Table 5.

DMD Fast Forward. Published on March 17, 2017 as DOI: 10.1124/dmd.116.074492
This article has not been copyedited and formatted. The final version may differ from this version.

Discussion

In severe renal failure patients, plasma exposures of the conjugated metabolites of morinidazole, M7, M8-1, and M8-2 significantly increased by over 15-fold compared with healthy subjects, whereas the plasma exposure of morinidazole increased by only 50% (Zhong et al., 2014). In this study, similar changes were found in 5/6 nephrectomized rats (Fig. 3 and Table 2); hence, they were used to mimic the *in vivo* CRF condition for further investigation of the relationship between pharmacokinetic alterations and transporters. Biochemistry parameters and histopathological sections showed that the CRF model was successfully constructed.

Sulfate conjugate M7 was synthesized to directly evaluate the pharmacokinetics in 5/6 Nx and control rats, excluding the influence of the metabolism from morinidazole to M7. N^+-glucuronide conjugates were difficult to synthesize; hence, the pharmacokinetics of M8-1 and M8-2 were not directly assessed. Compared with control rats, the plasma clearance of M7 in 5/6 Nx rats significantly decreased to 27.8%, whereas the MRT and AUC_{0-t} values increased by 3.05- and 3.61-fold, respectively (Table 3). These data further indicated that renal impairment in the 5/6 nephrectomized rats caused decelerated elimination of M7. Therefore, the plasma exposure was increased. Considering that the AUC value of M7 was elevated but morinidazole was not, the changes of transporters related to M7 were investigated.

In 5/6 Nx rats, mRNA expression of Oat1 and Oat3 decreased to approximately 50% (Fig. 6A and 6B). To further confirm whether the decreased mRNA levels of transporters induced the changes in the uptakes of the conjugated metabolites, experiments on fresh kidney slices

from 5/6 Nx and control rats were conducted. Accumulations of the three conjugated metabolites increased over time but showed no significant difference between control and 5/6 Nx kidney slices (Fig. 8A, 8B, and 8C). Although the mRNA expression decreased, the activities of two transporters presented no apparent effect on the uptakes of the conjugated metabolites. As a result, the down-regulated expression of transporters may not induce the increase in the plasma exposures of morinidazole-conjugated metabolites.

Recent studies have shown that protein-bound uremic toxins increased abnormally in the plasma of CRF patients (Vanholder et al., 2003; Fujita et al., 2011; Itoh et al., 2012). Some of these uremic toxins were proved to be substrates of renal transporters, OAT1 or OAT3 (Deguchi et al., 2004). In the present study, IS, HA, and IAA could be determined in 5/6 Nx rats. Correlation was found between the AUC values of M7 and plasma concentrations of IS or HA, but no correlation was observed between the AUC and the plasma concentration of IAA (Fig. 7). Therefore, IS, HA and their mixture were used to evaluate their effects on the renal uptakes of M7, M8-1, and M8-2. As shown in Fig. 8 (D, E, and F), individual and mixtures of IS and HA dose-dependently inhibited the uptakes of M7, M8-1, and M8-2 in normal fresh rat kidney slices, similar to the typical Oat inhibitor, probenecid (Emami Riedmaier et al., 2012).

In CRF patients, four highly elevated uremic toxins, CMPF, IS, HA, and IAA, were reported to reach 250, 210, 1400, and 5 μM in the plasma, respectively; and the maximum concentrations were 400, 940, 2600, and 50 μM, correspondingly; however, the concentrations were only 30, 2, 20, and 0.1 μM in healthy humans, respectively (Vanholder et al., 2003). Thus, these uremic toxins were used to investigate the effects on the uptakes of

DMD Fast Forward. Published on March 17, 2017 as DOI: 10.1124/dmd.116.074492
This article has not been copyedited and formatted. The final version may differ from this version.

three morinidazole-conjugated metabolites in OAT1- or OAT3-overexpressed HEK293 cells. In OAT3-overexpressed HEK293 cells, CMPF exhibited the highest inhibitory effect with IC_{50} values of 19.2 (M7), 8.53 (M8-1), and 6.75 μM (M8-2). These values were lower than the CMPF plasma concentration in CRF patients. The IC_{50} values of HA were 87.4 (M7), 39.4 (M8-1), and 24.1 μM (M8-2), and the IC_{50} values of IS were 222 (M7), 161 (M8-1), and 78.3 μM (M8-2); these values were also lower than or similar to their plasma concentrations in CRF patients. Although the plasma concentration of IAA was increased by 50 times in CRF patients, its IC_{50} for three conjugated metabolites were much higher than its plasma concentration in the patients, thus its effect on the renal uptake and plasma exposures of the conjugates might be minor. The inhibition results indicated that the increased concentrations of CMPF, HA, and IS in CRF patients caused the inhibition of renal clearance of three conjugated metabolites, thereby boosting the plasma exposures of M7, M8-1, and M8-2. In OAT1-overexpressed cells, the IC_{50} values for M7 were as high as 200 (IS), 187 (CMPF), 162 (HA), and 197 μM (IAA). These data indicated that inhibition of four uremic toxins on the OAT1-mediated M7 uptake was weak, although uremic toxins were reported to be inhibitors of some other substrates of OAT1 (Tsutsumi et al., 2002; Deguchi et al., 2004; Nigam et al., 2015a). This also means that CMPF, HA and IS inhibited the renal uptake of M7 mainly because of their inhibitory effects on OAT3 but not OAT1. This could explain the similar elevated folds of AUC values between M7 and M8-1 or M8-2 in renal impairment patients, although M7 was the substrate of OAT1 and OAT3 and M8-1 or M8-2 was substrate of only OAT3. The inhibitory mechanism of uremic toxins needs further research. Recent metabolomic data from *Oat3*-knockout mice and in vitro studies supported the viewpoint that

DMD Fast Forward. Published on March 17, 2017 as DOI: 10.1124/dmd.116.074492
This article has not been copyedited and formatted. The final version may differ from this version.

OAT3 is a major elimination route for many phase 2 metabolites, such as the glucuronides (Wu et al., 2013; Nigam et al., 2015b). The inhibitory effect of the uremic toxins on OAT could lead to the potential disposition alterations of drugs and conjugated metabolites in kidney disease.

The AUC value of M7 increased by 12.9-fold in 5/6 Nx rats after an intravenous injection of morinidazole. By contrast, the AUC value of M7 increased by only 3.61-fold in 5/6 Nx rats after a direct intravenous injection of M7. After M7 is directly administered to rats, their kidney concentrations were much higher (> 1000-fold) than those in rats receiving morinidazole. Therefore, it was inferred that the kidney uptakes of M7 may be saturated or inhibited at higher M7 concentrations, which can explain different increase trends of M7 plasma exposure in 5/6 Nx rats after intravenous injection of M7 and morinidazole, respectively.

Conjugated metabolism was not only a major elimination route of xenobiotics, some conjugated metabolites also exerted pharmacological or adverse effects. For instance, glucuronide conjugate of gemfibrozil was a stronger inhibitor of CYP2C8 than the parent drug, which might cause rhabdomyolysis (Ogilvie et al., 2006); morphine-6β-glucuronide was a more potent opioid agonist than morphine (Frances et al., 1992); and the sulfate of minoxidil demonstrated hypotensive effect similar to the parent drug (Meisheri et al., 1988). Therefore, the mechanisms of the changes in pharmacokinetics of the conjugated metabolites should be considered.

Increased evidence has reported that the alteration of endogenous substances in disease conditions might not only cause related syndrome, but have indirect (down-regulation) and

DMD Fast Forward. Published on March 17, 2017 as DOI: 10.1124/dmd.116.074492
This article has not been copyedited and formatted. The final version may differ from this version.

direct effects on transporters and metabolic enzymes. For instance, one of the bile acids, taurolithocholic acid (TLCA), which might increase in hepatic and intestinal diseases, exhibited strong inhibitory effects on UDP-glucuronosyltransferases (UGTs), and subsequently induced possible metabolic disorders (Fang et al., 2013). Clarification of the influential mechanism might provide some basis for therapeutic managements. This study suggested that in CRF patients, decreasing uremic toxin levels might help to reverse the altered pharmacokinetics of morinidazole-conjugated metabolites.

In conclusion, although the mRNA expression levels of Oat1 and Oat3 decreased in 5/6 Nx rats, their activities were not significantly affected. Accumulations of CMPF (only detected in humans), HA and IS, which were caused by renal impairment in humans and rats, inhibited the OAT3-mediated uptake of sulfate or N^+-glucuronides in the kidney, leading to deceleration of renal excretion and consequent elevation in plasma exposure. Therefore, in disease conditions, we should not solely focus on the expression changes of transporters or metabolizing enzymes but should also consider the influence of altered endogenous substances on the activities of these transporters or metabolizing enzymes.

Acknowledgements

We greatly appreciate Dr. Guoyu Pan (Shanghai Institute of Materia Medica, Chinese Academy of Sciences) for providing the Krumdieck tissue slicer MD6000, as well as Le Wang for his help with the instrument usage.

Authorship Contributions

Participated in research design: Kong, Chen.

Conducted experiments: Kong, Pang, K. Zhong, Guo, Li.

Contributed new reagents or analytic tools: Kong, Pang, D. Zhong, Chen.

Performed data analysis: Kong, Pang, Chen.

Wrote or contributed to the writing of the manuscript: Kong, Chen.

Conflicts of interest

The authors declare no conflicts of interest.

References

Anderson S, Meyer TW, Rennke HG, and Brenner BM (1985) Control of glomerular hypertension limits glomerular injury in rats with reduced renal mass. *J Clin Invest* **76:**612-619.

Deguchi T, Kusuhara H, Takadate A, Endou H, Otagiri M, and Sugiyama Y (2004) Characterization of uremic toxin transport by organic anion transporters in the kidney. *Kidney Int* **65:**162-174.

Deguchi T, Nakamura M, Tsutsumi Y, Suenaga A, and Otagiri M (2003) Pharmacokinetics and tissue distribution of uraemic indoxyl sulphate in rats. *Biopharm Drug Dispos* **24:**345-355.

Emami Riedmaier A, Nies AT, Schaeffeler E, and Schwab M (2012) Organic anion transporters and their implications in pharmacotherapy. *Pharmacol Rev* **64:**421-449.

Fang ZZ, He RR, Cao YF, Tanaka N, Jiang C, Krausz KW, Qi Y, Dong PP, Ai CZ, Sun XY, Hong M, Ge GB, Gonzalez FJ, Ma XC, and Sun HZ (2013) A model of in vitro UDP-glucuronosyltransferase inhibition by bile acids predicts possible metabolic disorders. *J Lipid Res* **54:**3334-3344.

Frances B, Gout R, Monsarrat B, Cros JEAN, and Zajac JM (1992) Further evidence that morphine-6 beta-glucuronide is a more potent opioid agonist than morphine. *J Pharmacol Exp Ther* **262:**25-31.

Fujita K, Sunakawa Y, Miwa K, Akiyama Y, Sugiyama M, Kawara K, Ishida H, Yamashita K, Mizuno K, Saji S, Ichikawa W, Yamamoto W, Nagashima F, Miya T, Narabayashi M, Ando Y, Hirose T, and Sasaki Y (2011) Delayed elimination of SN-38 in cancer

patients with severe renal failure. *Drug Metab Dispos* **39:**161-164.

Gao R, Li L, Xie C, Diao X, Zhong D, and Chen X (2011) Metabolism and Pharmacokinetics of Morinidazole in Humans: Identification of Diastereoisomeric Morpholine N+-Glucuronides Catalyzed by UDP Glucuronosyltransferase 1A9. *Drug Metab Dispos* **40:**556-567.

Habu Y, Yano I, Takeuchi A, Saito H, Okuda M, Fukatsu A, and Inui K-i (2003) Decreased activity of basolateral organic ion transports in hyperuricemic rat kidney: roles of organic ion transporters, rOAT1, rOAT3 and rOCT2. *Biochem Pharmacol* **66:**1107-1114.

Itoh Y, Ezawa A, Kikuchi K, Tsuruta Y, and Niwa T (2012) Protein-bound uremic toxins in hemodialysis patients measured by liquid chromatography/tandem mass spectrometry and their effects on endothelial ROS production. *Anal Bioanal Chem* **403:**1841-1850.

Kikuchi K, Itoh Y, Tateoka R, Ezawa A, Murakami K, and Niwa T (2010) Metabolomic analysis of uremic toxins by liquid chromatography/electrospray ionization-tandem mass spectrometry. *J Chromatogr B* **878:**1662-1668.

Livak KJ and Schmittgen TD (2001) Analysis of relative gene expression data using real-time quantitative PCR and the 2(-Delta Delta C(T)) Method. *Methods* **25:**402-408.

Meisheri KD, Cipkus LA, and Taylor CJ (1988) Mechanism of action of minoxidil sulfate-induced vasodilation: a role for increased K+ permeability. *J Pharmacol Exp Ther* **245:**751-760.

Moll S, Meier M, Formentini I, Pomposiello S, and Prunotto M (2014) New renal drug development to face chronic renal disease. *Expert Opin Drug Discov* **9:**1471-1485.

Naud J, Michaud J, Beauchemin S, Hebert MJ, Roger M, Lefrancois S, Leblond FA, and Pichette V (2011) Effects of Chronic Renal Failure on Kidney Drug Transporters and Cytochrome P450 in Rats. *Drug Metab Dispos* **39:**1363-1369.

Nigam SK (2015) What do drug transporters really do? *Nat Rev Drug Discov* **14:**29-44.

Nigam SK, Bush KT, Martovetsky G, Ahn SY, Liu HC, Richard E, Bhatnagar V, and Wu W (2015a) The organic anion transporter (OAT) family: a systems biology perspective. *Physiol Rev* **95:**83-123.

Nigam SK, Wu W, Bush KT, Hoenig MP, Blantz RC, and Bhatnagar V (2015b) Handling of Drugs, Metabolites, and Uremic Toxins by Kidney Proximal Tubule Drug Transporters. *Clin J Am Soc Nephrol* **10:**2039-2049.

Obatomi DK, Brant S, Anthonypillai V, Early DA, and Bach PH (1998) Optimizing preincubation conditions for precision-cut rat kidney and liver tissue slices: effect of culture media and antioxidants. *Toxicol In Vitro* **12:**725-737.

Ogilvie BW, Zhang D, Li W, Rodrigues AD, Gipson AE, Holsapple J, Toren P, and Parkinson A (2006) Glucuronidation converts gemfibrozil to a potent, metabolism-dependent inhibitor of CYP2C8: implications for drug-drug interactions. *Drug Metab Dispos* **34:**191-197.

Periclou A, Ventura D, Rao N, and Abramowitz W (2006) Pharmacokinetic study of memantine in healthy and renally impaired subjects. *Clin Pharmacol Ther* **79:**134-143.

Sakurai Y, Motohashi H, Ueo H, Masuda S, Saito H, Okuda M, Mori N, Matsuura M, Doi T, Fukatsu A, Ogawa O, and Inui KI (2004) Expression levels of renal organic anion

transporters (OATs) and their correlation with anionic drug excretion in patients with renal diseases. *Pharm Res* **21:**61-67.

Sarnatskaya VV, Lindup WE, Niwa T, Ianov AI, Yushko LA, Tjia J, Maslenny VN, Korneeva LN, and Nikolaev VG (2002) Effect of protein-bound uraemic toxins on the thermodynamic characteristics of human albumin. *Biochem Pharmacol* **63:**1287-1296.

Schwenk MH and Pai AB (2016) Drug Transporter Function--Implications in CKD. *Adv Chronic Kidney Dis* **23:**76-81.

Shrestha SL, Bai X, Smith DJ, Hakk H, Casey FX, Larsen GL, and Padmanabhan G (2011) Synthesis and characterization of radiolabeled 17β-estradiol conjugates. *J Labelled Compd Radiopharmaceut* **54:**267-271.

Tsutsumi Y, Deguchi T, Takano M, Takadate A, Lindup WE, and Otagiri M (2002) Renal disposition of a furan dicarboxylic acid and other uremic toxins in the rat. *J Pharmacol Exp Ther* **303:**880-887.

Vanholder R, De Smet R, Glorieux G, Argilés A, Baurmeister U, Brunet P, Clark W, Cohen G, De Deyn PP, Depposch R, Descamps-Latscha B, Henle T, Jörres A, Lemke HD, Massy ZA, Passlick-Deetjen J, Rodriguez M, Stegmayr B, Stenvinkel P, Tetta C, Wanner C, and Zidek W (2003) Review on uremic toxins: Classification, concentration, and interindividual variability. *Kidney Int* **63:**1934-1943.

Verbeeck RK and Musuamba FT (2009) Pharmacokinetics and dosage adjustment in patients with renal dysfunction. *Eur J Clin Pharmacol* **65:**757-773.

Wikoff WR, Nagle MA, Kouznetsova VL, Tsigelny IF, and Nigam SK (2011) Untargeted metabolomics identifies enterobiome metabolites and putative uremic toxins as

substrates of organic anion transporter 1 (Oat1). *J Proteome Res* **10:**2842-2851.

Wu W, Jamshidi N, Eraly SA, Liu HC, Bush KT, Palsson BO, and Nigam SK (2013) Multispecific drug transporter Slc22a8 (Oat3) regulates multiple metabolic and signaling pathways. *Drug Metab Dispos* **41:**1825-1834.

Zhong K, Li X, Xie C, Zhang Y, Zhong D, and Chen X (2014) Effects of renal impairment on the pharmacokinetics of morinidazole: uptake transporter-mediated renal clearance of the conjugated metabolites. *Antimicrob Agents Chemother* **58:**4153-4161.

Footnotes

This work was financially supported by Youth Innovation Promotion Association CAS.

Figure legends:

Fig. 1. Major metabolic pathways of morinidazole in humans.

Fig. 2. Histologic sections of renal glomerulus from control rat (A) and 5/6 Nx rat (C), renal tubules from control rat (B) and 5/6 Nx rat (D).

Fig. 3. Mean plasma drug concentration–time profiles of M0 (A), M7 (B), M8-1 (C), and M8-2 (D) following an intravenous administration of morinidazole (50 mg/kg) to control and 5/6 Nx rats.

Fig. 4. Mean plasma drug concentration–time profiles of M7 following an intravenous administration of M7 (15 mg/kg) to control and 5/6 Nx rats.

Fig. 5. Tissue distributions of M7 following intravenous administration of morinidazole (A) and M7 (B) in rats, respectively.

Fig. 6. mRNA expression of renal transporter Oat1 (A) and Oat3 (B) in control (n=9) and 5/6 Nx (n=13) rats. Correlation between the $AUC_{0\text{-}t}$ values of M7 after intravenous administration of 15 mg/kg and mRNA expression of Oat1 (C) or Oat3 (D). ***, $p < 0.001$ compared with control.

Fig. 7. Concentrations of IS (A), HA (C), and IAA (E) in plasma and kidneys of control (n=9) and 5/6 Nx (n=13) rats. Correlation between the $AUC_{0\text{-}t}$ values of M7 (n=22) and plasma concentrations of IS (B), HA (D) or IAA (F). **, $p < 0.01$, ***, $p < 0.001$ compared with control.

Fig. 8. Uptakes of M7 (A), M8-1 (B), and M8-2 (C) in the kidney slices of control (n=4) and 5/6 Nx rats (n=6) for 5 and 15 min. The inhibitory effect of HA, IS and their mixture with different concentration on the uptake of M7 (D), M8-1(E), and M8-2(F) in the kidney slices

from normal rats. *, $p < 0.05$, **, $p < 0.01$, ***, $p < 0.001$ compared with control.

Fig. 9. Inhibitory effects of four uremic toxins on the M7 (A) uptake in the OAT1-overexpressed HEK293 cells, M7 (B), M8-1 (C), and M8-2 (D) uptakes in the OAT3-overexpressed HEK293 cells. OAT1 and OAT3 mediated 30 μM M7 uptake for 1 min and OAT3 mediated 100 μM M8-1 uptake and 20 μM M8-2 uptake for 3 min were determined in the absence and presence of CMPF, IS, HA, and IAA at the designated concentrations. Transporter-mediated M7, M8-1, and M8-2 accumulations were corrected by subtracting the nonspecific accumulation in the mock-transfected HEK293 cells from that in the OAT-expressing HEK293 cells. The values were expressed as a percentage of the uptake in the absence of uremic toxins. Solid lines represent the fitted line obtained by nonlinear regression analysis. Each point was presented as mean ± SD (n=3).

DMD Fast Forward. Published on March 17, 2017 as DOI: 10.1124/dmd.116.074492
This article has not been copyedited and formatted. The final version may differ from this version.

Table 1. Biochemical parameters of control and 5/6 Nx rats.

Parameter	Control rats (n=19)	5/6 Nx rats (n=34)
Body Weight (g)	379 ± 32	313 ± 32***
Serum BUN (mM)	6.91 ± 8.14	49.0 ± 23.7***
Serum Creatinine (μM)	40.6 ± 34.2	117 ± 62**
Urinary protein excretion (mg/day)	16.1 ± 3.5	54.7 ± 54.9*
Creatinine clearance (mL/kg body weight/min)	16.8 ± 17.7	4.45 ± 3.55*

Data were expressed as mean ± SD. * $p < 0.05$, ** $p < 0.01$, *** $p < 0.001$ compared with control.

DMD Fast Forward. Published on March 17, 2017 as DOI: 10.1124/dmd.116.074492
This article has not been copyedited and formatted. The final version may differ from this version.

Table 2. Pharmacokinetic parameters of morinidazole and its major metabolites following an intravenous administration of 50 mg/kg of morinidazole to control (n=6) and 5/6 Nx (n=11) rats.

Group	Pharmacokinetic parameter[a]	Morinidazole M0	Sulfate conjugate M7	Glucuronide conjugates M8-1	Glucuronide conjugates M8-2
Control rat	C_{max} (μg/mL)	48.2 ± 6.1	0.00928 ± 0.00337	0.0988 ± 0.0134	0.356 ± 0.087
	t_{max} (h)	0.08 ± 0.00	0.46 ± 0.29	0.75 ± 0.27	1.00 ± 0.00
	$t_{1/2}$ (h)	1.16 ± 0.09	1.24 ± 0.34	0.94 ± 0.11	1.49 ± 0.28
	AUC_{0-t} (μg·h/mL)	87.2 ± 11.7	0.0164 ± 0.0076	0.257 ± 0.037	1.12 ± 0.36
	$AUC_{0-\infty}$ (μg·h/mL)	87.3 ± 11.7	0.0177 ± 0.0081	0.257 ± 0.037	1.12 ± 0.36
	CL (mL/h/kg)	582 ± 77			
	V_{ss} (mL/kg)	805 ± 71			
	MRT (h)	1.39 ± 0.12	1.75 ± 0.33	1.86 ± 0.22	2.21 ± 0.38
5/6 Nx rats	C_{max} (μg/mL)	53.2 ± 3.5*	0.0828 ± 0.0293***	0.810 ± 0.680*	4.25 ± 2.68**
	t_{max} (h)	0.08 ± 0.00	0.82 ± 0.25*	1.64 ± 0.50***	1.91 ± 0.30***
	$t_{1/2}$ (h)	1.32 ± 0.08**	1.88 ± 0.79	1.06 ± 0.08*	1.28 ± 0.11
	AUC_{0-t} (μg·h/mL)	91.2 ± 8.7	0.211 ± 0.081***	2.76 ± 2.36*	15.7 ± 10.0**
	$AUC_{0-\infty}$ (μg·h/mL)	91.3 ± 8.7	0.214 ± 0.081***	2.76 ± 2.36*	15.7 ± 10.0**
	CL (mL/h/kg)	552 ± 50			
	V_{ss} (mL/kg)	891 ± 41**			
	MRT (h)	1.62 ± 0.12**	2.13 ± 0.13*	2.30 ± 0.19**	2.65 ± 0.22**

[a] C_{max}, maximum plasma concentration; t_{max}, time to the C_{max}. $t_{1/2}$, apparent elimination

half-life; AUC_{0-t}, area under the concentration-time curve from 0 h to the last sampling time; $AUC_{0-\infty}$, area under the concentration-time curve from 0 h to the infinite time; CL, total body clearance; V_{SS}, volume of distribution at steady state; MRT, mean residence time. Data were expressed as mean ± SD. * $p < 0.05$, ** $p < 0.01$, *** $p < 0.001$ compared with control.

DMD Fast Forward. Published on March 17, 2017 as DOI: 10.1124/dmd.116.074492
This article has not been copyedited and formatted. The final version may differ from this version.

Table 3. Pharmacokinetic parameters of M7 following an intravenous administration of 15 mg/kg M7 to control (n=9) and 5/6 Nx (n=13) rats.

	Control rats (n=9)	5/6 Nx rats (n=13)
C_{max} (μg/mL)	24.7 ± 6.4	51.9 ± 7.4***
t_{max} (h)	0.08 ± 0.00	0.08 ± 0.00
$t_{1/2}$ (h)	0.27 ± 0.05	0.93 ± 0.29***
AUC_{0-t} (μg·h/mL)	7.83 ± 1.71	28.3 ± 6.9***
$AUC_{0-\infty}$ (μg·h/mL)	7.87 ± 1.71	28.5 ± 6.9***
CL (L/h/kg)	1.98 ± 0.41	0.55 ± 0.11***
V_{ss} (L/kg)	0.40 ± 0.15	0.33 ± 0.08
MRT (h)	0.20 ± 0.05	0.61 ± 0.17***

Data were expressed as mean ± SD. *** $p < 0.001$ compared with control.

DMD Fast Forward. Published on March 17, 2017 as DOI: 10.1124/dmd.116.074492
This article has not been copyedited and formatted. The final version may differ from this version.

Table 4. Pharmacokinetic parameters of M7 with intravenous administration of different dose in normal rats.

	0.1 mg/kg	1.5 mg/kg	15 mg/kg
C_{max} (μg/mL)	0.0820 ± 0.0122	1.53 ± 0.15	14.1 ± 2.7
t_{max} (h)	0.08 ± 0.00	0.08 ± 0.00	0.08 ± 0.00
$t_{1/2}$ (h)	0.26 ± 0.05	0.22 ± 0.03	0.24 ± 0.02
AUC_{0-t} (μg·h/mL)	0.0233 ± 0.0039	0.426 ± 0.043	4.09 ± 0.72
$AUC_{0-\infty}$ (μg·h/mL)	0.0235 ± 0.0039	0.427 ± 0.043	4.10 ± 0.72
CL (L/h/kg)	4.36 ± 0.76	3.54 ± 0.34	3.75 ± 0.69
V_{ss} (L/kg)	0.63 ± 0.09	0.45 ± 0.04	0.58 ± 0.15
MRT (h)	0.15 ± 0.02	0.13 ± 0.01	0.16 ± 0.02

Data were expressed as mean ± SD. n=4.

DMD Fast Forward. Published on March 17, 2017 as DOI: 10.1124/dmd.116.074492
This article has not been copyedited and formatted. The final version may differ from this version.

Table 5. IC_{50} values of uremic toxins on the inhibition of morinidazole conjugates uptake in OAT expressed HEK293 cells.

Substrate	Transporter	IC_{50} values of inhibitors (μM)			
		IS	CMPF	HA	IAA
M7	OAT1	200 ± 42	187 ± 22	162 ± 17	197 ± 26
M7	OAT3	222 ± 28	19.2 ± 1.3	87.4 ± 6.0	404 ± 33
M8-1	OAT3	161 ± 38	8.53 ± 0.31	39.4 ± 1.8	181 ± 7
M8-2	OAT3	78.3 ± 12.7	6.75 ± 1.76	24.1 ± 2.3	173 ± 33

Data were expressed as mean ± SD. n=3.

DMD Fast Forward. Published on March 17, 2017 as DOI: 10.1124/dmd.116.074492
This article has not been copyedited and formatted. The final version may differ from this version.

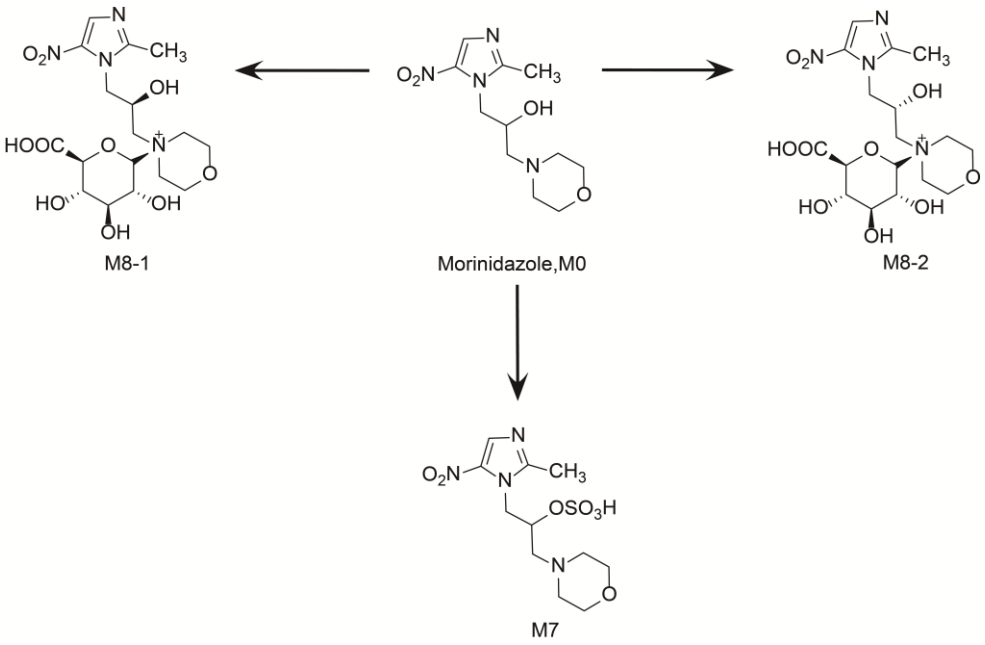

Fig. 1

DMD Fast Forward. Published on March 17, 2017 as DOI: 10.1124/dmd.116.074492
This article has not been copyedited and formatted. The final version may differ from this version.

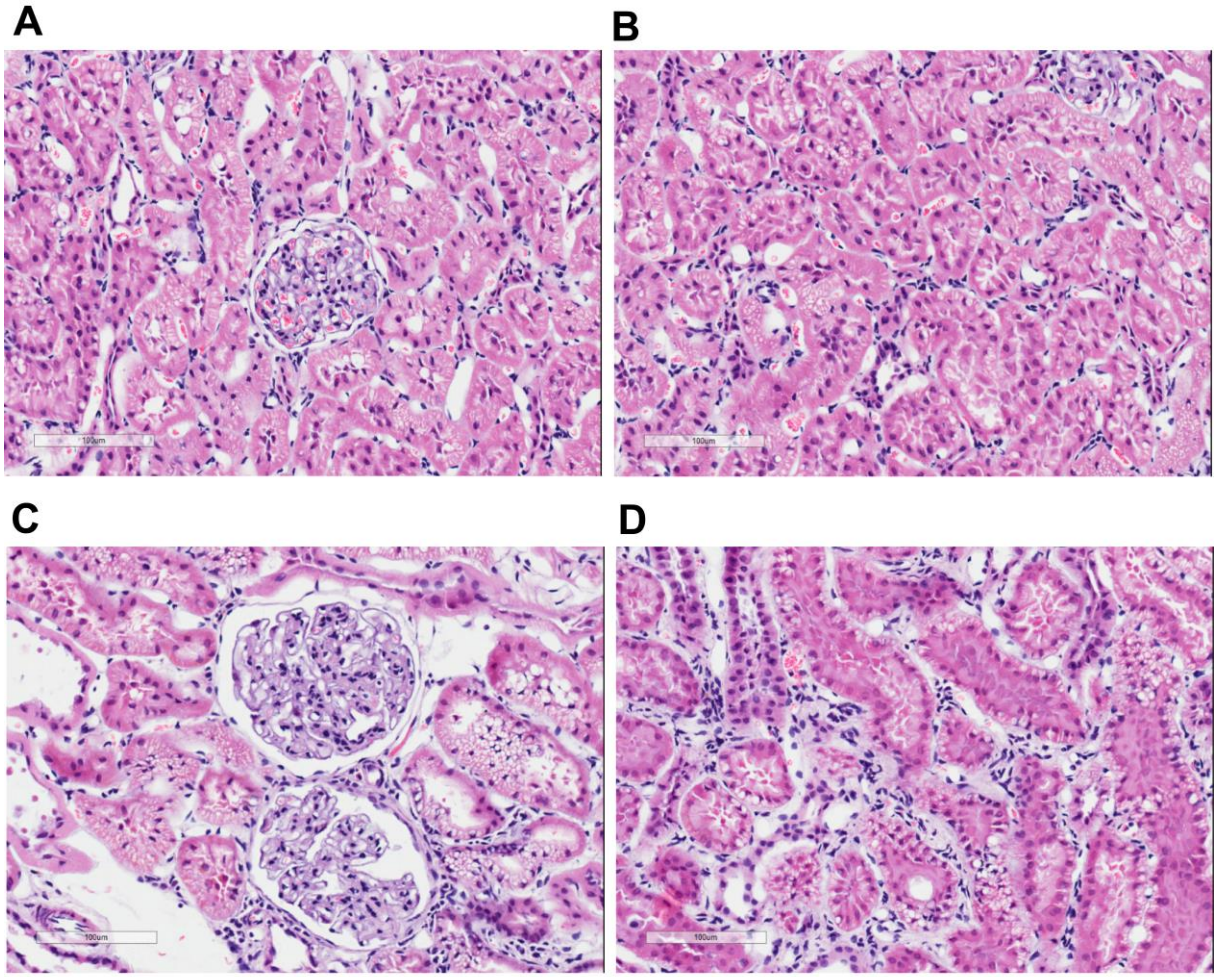

Fig. 2

DMD Fast Forward. Published on March 17, 2017 as DOI: 10.1124/dmd.116.074492
This article has not been copyedited and formatted. The final version may differ from this version.

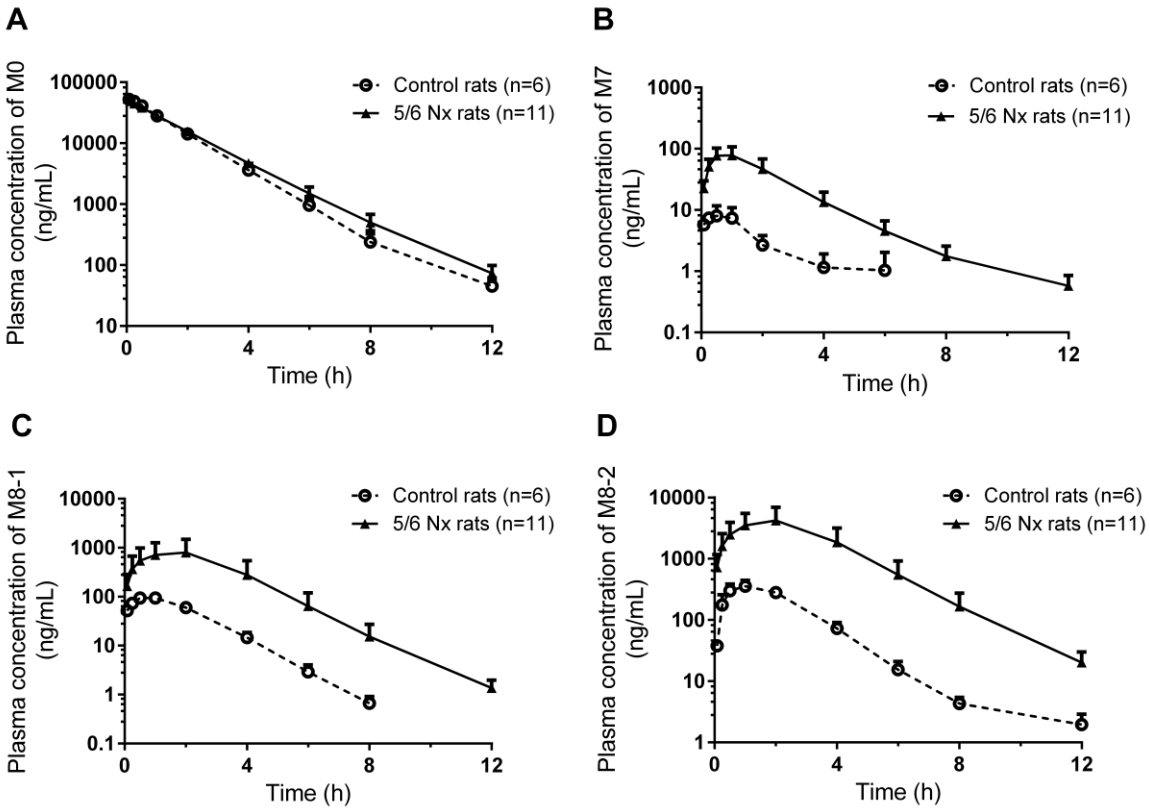

Fig. 3

DMD Fast Forward. Published on March 17, 2017 as DOI: 10.1124/dmd.116.074492
This article has not been copyedited and formatted. The final version may differ from this version.

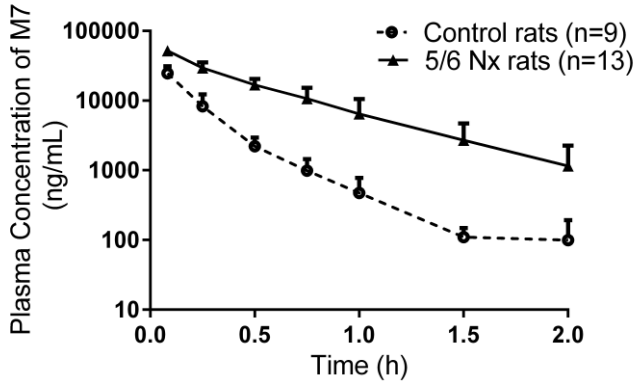

Fig. 4

DMD Fast Forward. Published on March 17, 2017 as DOI: 10.1124/dmd.116.074492
This article has not been copyedited and formatted. The final version may differ from this version.

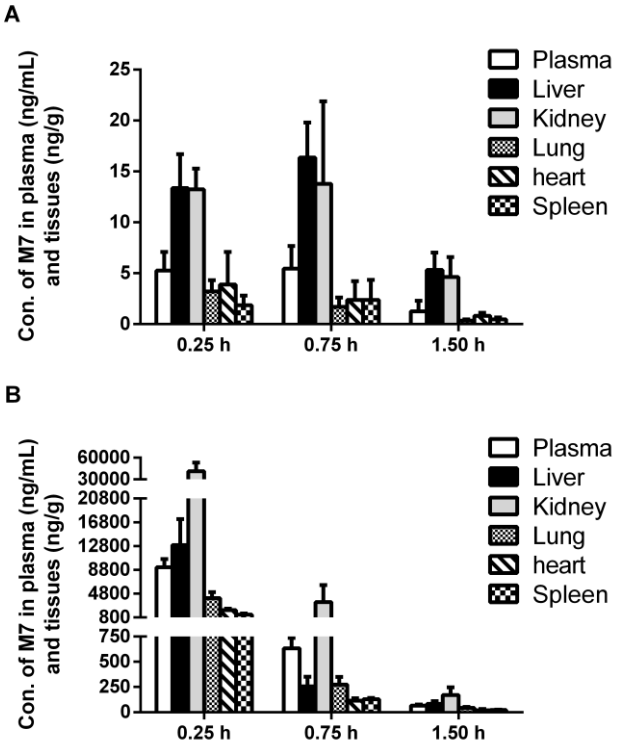

Fig. 5

DMD Fast Forward. Published on March 17, 2017 as DOI: 10.1124/dmd.116.074492
This article has not been copyedited and formatted. The final version may differ from this version.

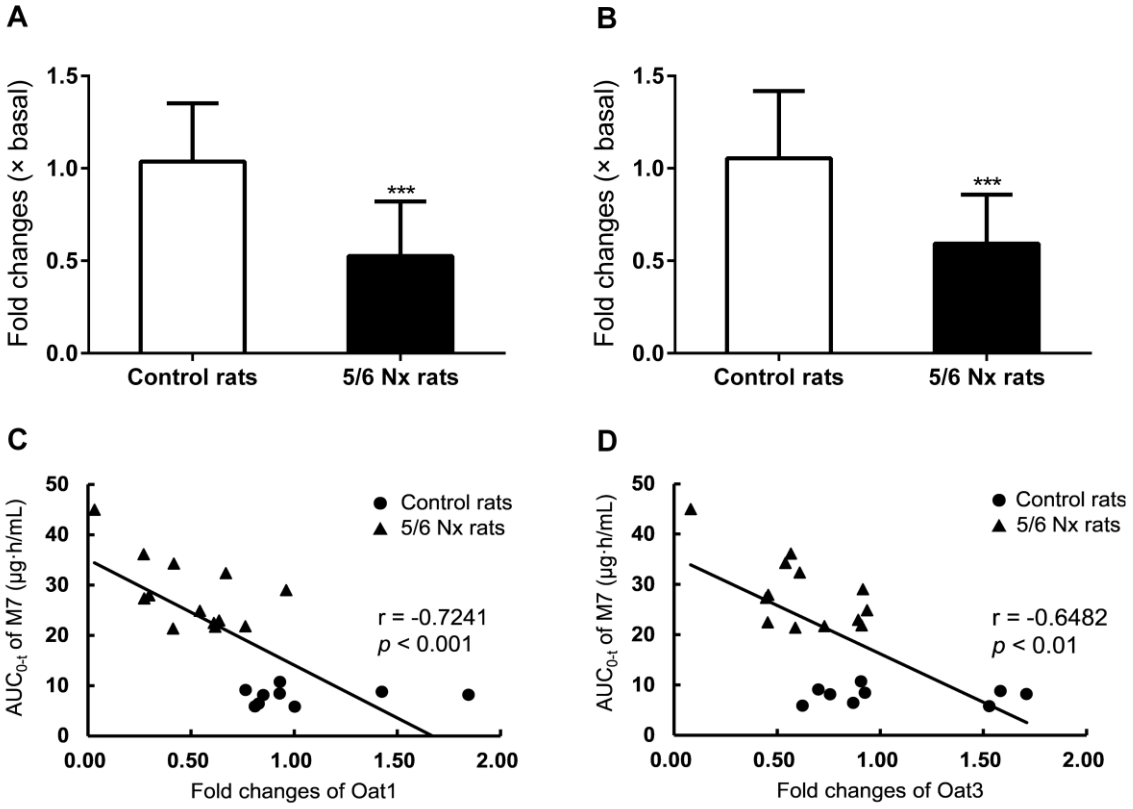

Fig. 6

DMD Fast Forward. Published on March 17, 2017 as DOI: 10.1124/dmd.116.074492
This article has not been copyedited and formatted. The final version may differ from this version.

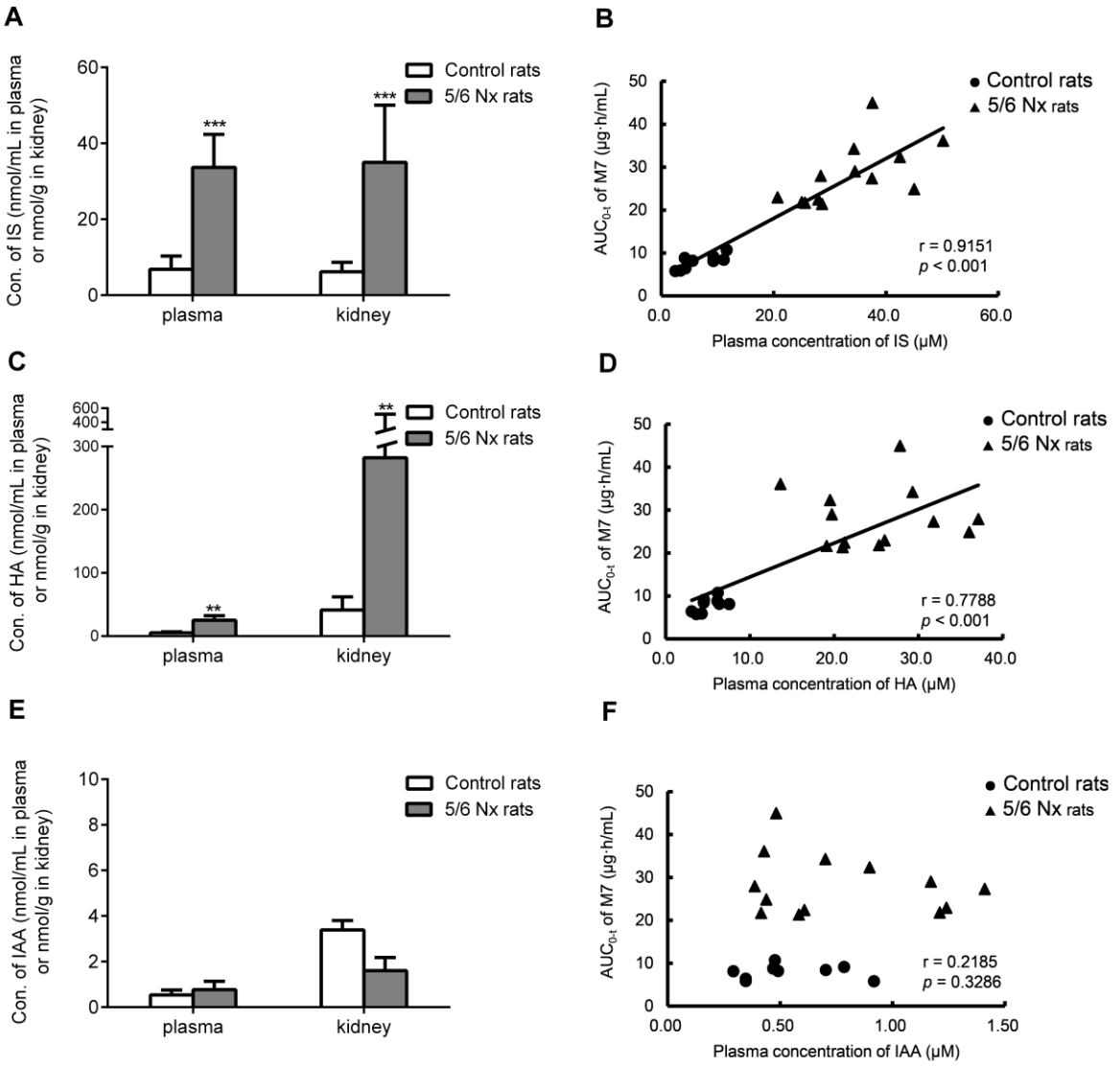

Fig. 7

DMD Fast Forward. Published on March 17, 2017 as DOI: 10.1124/dmd.116.074492
This article has not been copyedited and formatted. The final version may differ from this version.

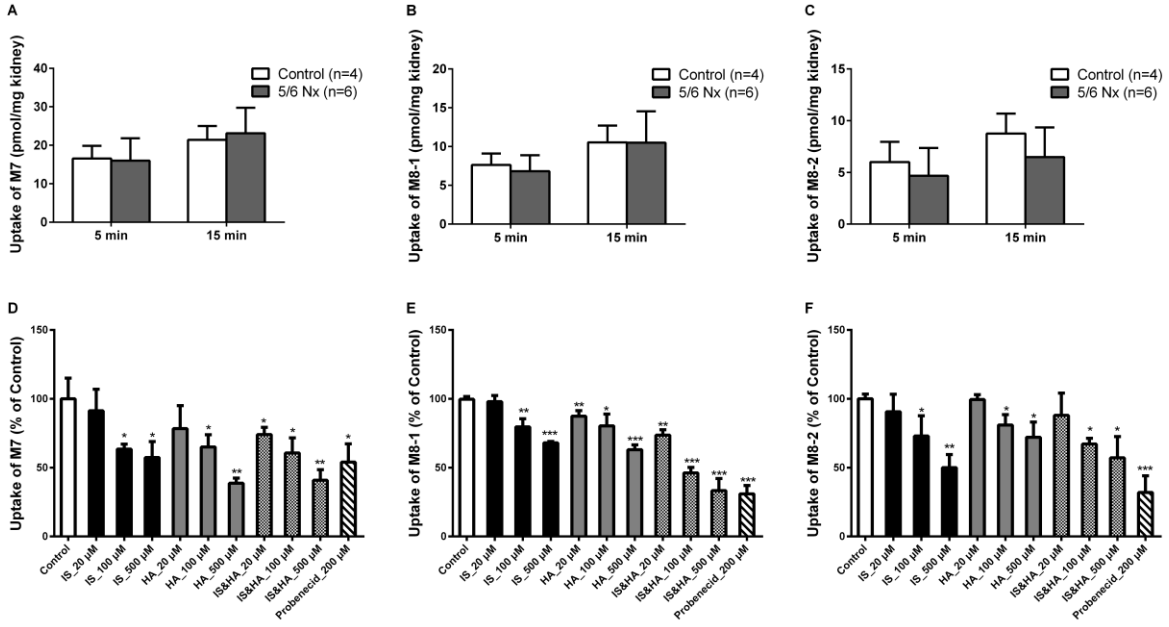

Fig.8

DMD Fast Forward. Published on March 17, 2017 as DOI: 10.1124/dmd.116.074492
This article has not been copyedited and formatted. The final version may differ from this version.

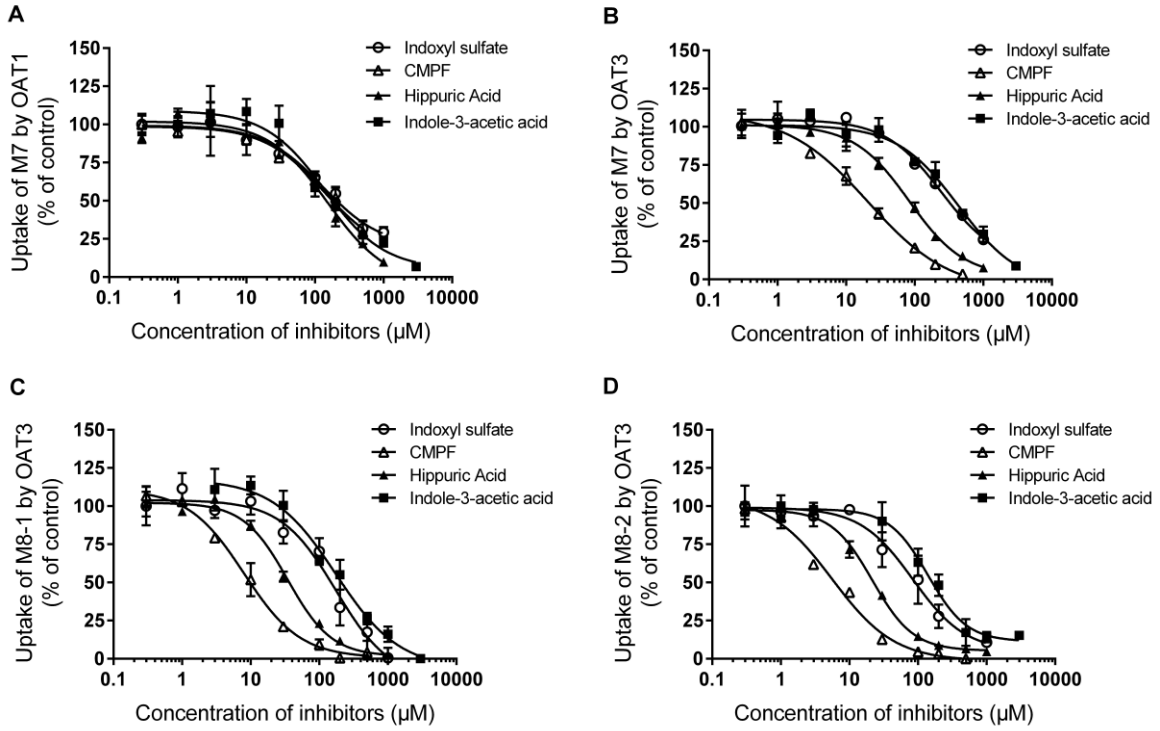

Fig. 9

Supplemental Data

Increased Plasma Exposures of Conjugated Metabolites of Morinidazole in Renal Failure Patients: A Critical Role of Uremic Toxins

Fandi Kong, Xiaoyan Pang, Kan Zhong, Zitao Guo, Xiuli Li, Dafang Zhong, and Xiaoyan Chen

Drug Metabolism and Disposition

Supplemental figure 1. Inhibitions of four uremic toxins mixtures or probenecid (200 μM) on the M7(A) uptake in the OAT1-overexpressed HEK293 cells; M7(B), M8-1(C), and M8-2(D) uptakes in the OAT3-overexpressed HEK293 cells. The concentrations of CMPF, IS, HA, and IAA were 10, 10, 10, and 1 μM for mix 1; 30, 30, 30, and 3 μM for mix 2; 100, 100, 100, and 10 μM for mix 3; and 300, 1000, 3000, and 100 μM for mix 4. The incubation period was 1 min for M7 and 3 min for M8-1 and M8-2. Transporter-mediated M7, M8-1, and M8-2 accumulations were corrected by subtracting the nonspecific accumulation in the mock-transfected HEK293 cells from that in the OAT overexpressed HEK293 cells. The values were expressed as a percentage of the uptake in the absence of uremic toxins. Each uptake value is represented as mean ± SD (n = 3). ***, $p < 0.001$ compared with control.

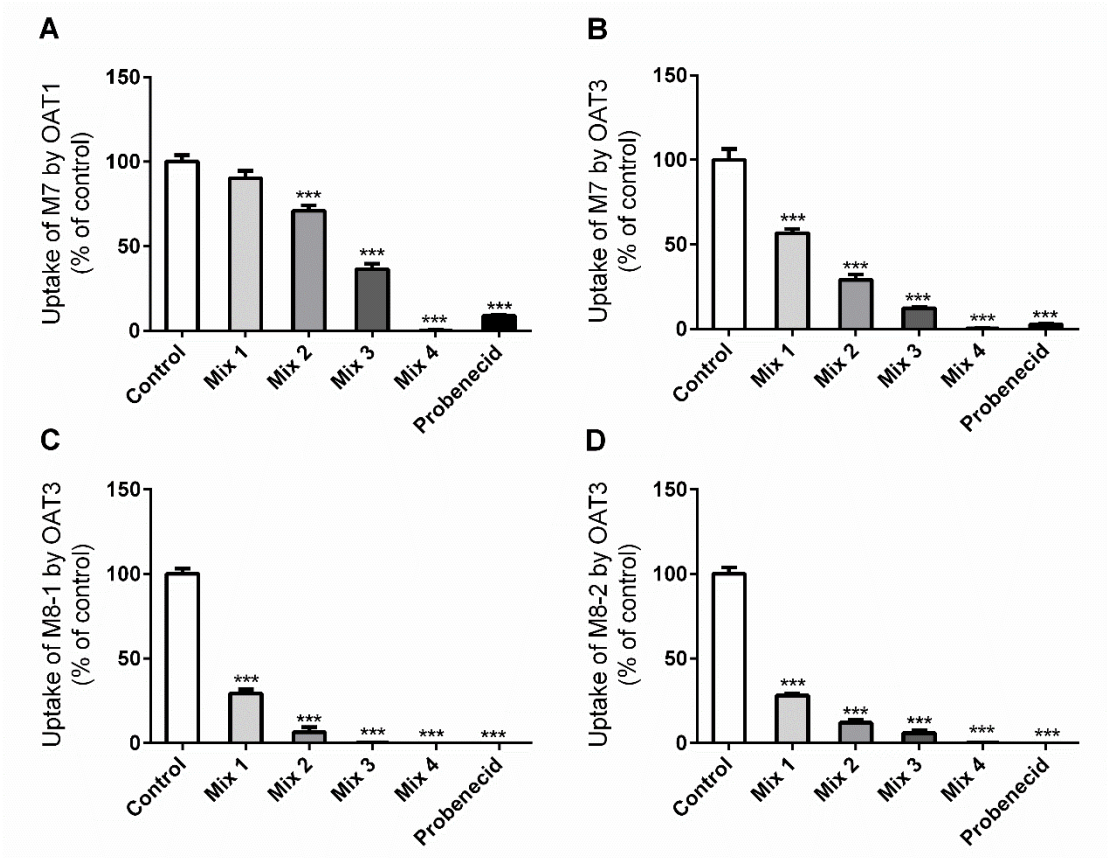

Supplemental Figure.1